

UCD-96-15

University of California - Davis

July, 1996

Revised: April, 1997

Prospects for and Implications of Measuring the Higgs to Photon-Photon  
Branching Ratio at the Next Linear  $e^+e^-$  Collider

John F. Gunion and Patrick C. Martin

*Davis Institute for High Energy Physics**Department of Physics, University of California, Davis, CA 95616*

### Abstract

We evaluate the prospects for measuring  $B(h \rightarrow \gamma\gamma)$  for a Standard-Model-like Higgs boson at the Next Linear  $e^+e^-$  Collider in the  $e^+e^- \rightarrow Z^* \rightarrow Zh$  and  $e^+e^- \rightarrow \nu_e \bar{\nu}_e h$  production modes. Relative merits of different machine energy/luminosity strategies and different electromagnetic calorimeter designs are evaluated. We emphasize the importance of measuring  $B(h \rightarrow \gamma\gamma)$  in order to obtain the total width of a light Higgs boson and thereby the  $b\bar{b}$  partial width that will be critical in discriminating between the SM Higgs and the Higgs bosons of an extended model.

### I. INTRODUCTION

One of the most important tasks of a Next Linear  $e^+e^-$  Collider (NLC) will be to detect and study Higgs boson(s). For any observed Higgs boson, extraction of its fundamental couplings and total width in a model-independent manner will be a primary goal. Measurement of  $B(h \rightarrow \gamma\gamma)$  turns out to be an absolutely necessary ingredient in extracting

the total width and  $b\bar{b}$  coupling in the case of a light Higgs boson with mass  $\lesssim 130$  GeV\* and couplings similar to those of the Standard Model (SM) Higgs,  $h_{SM}$ , and therefore a total width that is too small to be directly observed. The procedure for obtaining the total and  $b\bar{b}$  partial widths using  $B(h \rightarrow \gamma\gamma)$  is the following:

- Determine  $B(h \rightarrow b\bar{b})$  in  $e^+e^- \rightarrow Z^* \rightarrow Zh$  and  $e^+e^- \rightarrow e^+e^-h$  ( $ZZ$ -fusion) from the ratios  $B(h \rightarrow b\bar{b}) = [\sigma(Zh)B(h \rightarrow b\bar{b})]/\sigma(Zh)$  (with  $Z \rightarrow \ell^+\ell^-$ ,  $\ell = e, \mu$ ) and  $B(h \rightarrow b\bar{b}) = [\sigma(e^+e^-h)B(h \rightarrow b\bar{b})]/\sigma(e^+e^-h)$ , respectively. For  $L = 200$  fb $^{-1}$  of data at  $\sqrt{s} = 500$  GeV, the error for  $B(h \rightarrow b\bar{b})$  would be about  $\pm 5\%$  [1].
- Measure at the associated  $\gamma\gamma$  collider facility the rate for  $\gamma\gamma \rightarrow h \rightarrow b\bar{b}$  (accuracy  $\sim \pm 8\%$  [1] for  $L = 50$  fb $^{-1}$ ) proportional to  $\Gamma(h \rightarrow \gamma\gamma)B(h \rightarrow b\bar{b})$  and compute (accuracy  $\sim \pm 13\%$ )  $\Gamma(h \rightarrow \gamma\gamma) = [\Gamma(h \rightarrow \gamma\gamma)B(h \rightarrow b\bar{b})]/B(h \rightarrow b\bar{b})$ .
- Measure  $B(h \rightarrow \gamma\gamma)$  as described shortly, and then compute:

$$\Gamma_h^{\text{tot}} = \frac{\Gamma(h \rightarrow \gamma\gamma)}{B(h \rightarrow \gamma\gamma)}; \quad \text{and} \quad \Gamma(h \rightarrow b\bar{b}) = \Gamma_h^{\text{tot}} B(h \rightarrow b\bar{b}). \quad (1)$$

For a SM-like  $h$ , measurement of  $B(h \rightarrow \gamma\gamma)$  at the NLC will be challenging because of its small size (at best of order a few times  $10^{-3}$  [2]). One will measure  $[\sigma(e^+e^- \rightarrow Zh)B(h \rightarrow \gamma\gamma)]$ ,  $[\sigma(e^+e^- \rightarrow \nu_e\bar{\nu}_e h)B(h \rightarrow \gamma\gamma)]$  and  $[\sigma(e^+e^- \rightarrow \nu_e\bar{\nu}_e h)B(h \rightarrow b\bar{b})]$  (the latter two being  $WW$ -fusion processes) and compute  $B(h \rightarrow \gamma\gamma)$  via the  $Zh$  and  $WW$ -fusion ratios,

$$\frac{[\sigma(Zh)B(h \rightarrow \gamma\gamma)]}{\sigma(Zh)} \quad \text{and} \quad \frac{[\sigma(\nu_e\bar{\nu}_e h)B(h \rightarrow \gamma\gamma)]B(h \rightarrow b\bar{b})}{[\sigma(\nu_e\bar{\nu}_e h)B(h \rightarrow b\bar{b})]}, \quad (2)$$

respectively. Errors in the above two  $B(h \rightarrow \gamma\gamma)$  computations will be dominated by the errors in the  $\sigma B(h \rightarrow \gamma\gamma)$  measurements. (The  $e^+e^-h$  final state from  $ZZ$ -fusion provides a third alternative, but does not yield competitive errors because of a larger background.) Which of the ratios in Eq. (2) will yield the smallest errors for  $B(h \rightarrow \gamma\gamma)$  is dependent upon

---

\*For  $m_{h_{SM}} \gtrsim 130$  GeV, a 2nd technique based on  $WW^*$  decays emerges [1].

many factors. In this Letter, we assess the relative merits of the  $Zh$  and  $WW$ -fusion modes as a function of Higgs boson mass, machine energy, electromagnetic calorimeter resolution and luminosity/upgrade strategies.

The importance of a direct determination of  $\Gamma_h^{\text{tot}}$  and  $\Gamma(h \rightarrow b\bar{b})$  is due to the ambiguities associated with measuring only  $B(h \rightarrow b\bar{b})$ . Consider, for example, the light  $h^0$  of the minimal supersymmetric model (MSSM). Model parameter choices are easily found such that  $\Gamma(h^0 \rightarrow b\bar{b})$  is much larger than predicted for the  $h_{SM}$  [2], but  $B(h^0 \rightarrow b\bar{b})$  is only slightly larger than expected due to the fact that the numerator,  $\Gamma(h^0 \rightarrow b\bar{b})$ , and denominator,  $\Gamma_{h^0}^{\text{tot}}$ , are both increased by similar amounts. Extra (supersymmetric particle) decay modes could even enhance  $\Gamma_{h^0}^{\text{tot}}$  further, and  $B(h^0 \rightarrow b\bar{b})$  could be smaller than the SM prediction despite the fact that  $\Gamma(h^0 \rightarrow b\bar{b})$  is enhanced. Equation (1) shows that the ability to detect deviations of  $\Gamma_h^{\text{tot}}$  and  $\Gamma(h \rightarrow b\bar{b})$  from SM expectations depends critically on the error in  $B(h \rightarrow \gamma\gamma)$ , which is very likely to be the dominant source of uncertainty. Of course, dramatic deviations of  $B(h \rightarrow \gamma\gamma)$  from SM expectations are also a possibility, even if the  $h$  is very SM-like in its couplings to the SM particles. Large effects can be caused by new particles (fourth generation, supersymmetric, *etc.*) in the one-loop graphs responsible for the  $h \rightarrow \gamma\gamma$  coupling. Regardless of the size of the deviations from SM predictions, determining  $B(h \rightarrow \gamma\gamma)$  will be vital to understanding the nature of the Higgs boson and will provide an important probe of, or limits on, new physics that may lie beyond the SM.

## II. PROCEDURES

We consider SM Higgs masses in the range  $70 - 150$  GeV;  $B(h_{SM} \rightarrow \gamma\gamma)$  in units of  $10^{-3}$  is 0.75, 1.0, 1.4, 1.8, 2.2, 2.6, 2.6, 2.2, 1.6 as  $m_{h_{SM}}$  ranges from 70 to 150 GeV in steps of 10 GeV. In computing signals and backgrounds, we use exact matrix elements. To define  $Z\gamma\gamma$  vs.  $\nu_e\bar{\nu}_e\gamma\gamma$  events, we employ the recoil mass,  $M_X = \sqrt{(p_{e^+} + p_{e^-} - p_{\gamma_1} - p_{\gamma_2})^2}$ . We define  $Z\gamma\gamma$  events as  $X\gamma\gamma$  events for which  $M_X$  is within the interval  $[80, 100]$  (GeV). In this way, we can use all  $Z$  decay modes while ensuring that the only significant background

is that from  $Z\gamma\gamma$  non-Higgs diagrams. (Interference between signal and background  $Z\gamma\gamma$  diagrams is small.) The  $M_X$  cut also implies that for  $X = \nu_e\bar{\nu}_e$  the signal is almost entirely from  $Z^* \rightarrow Zh_{SM}$  (interference with the  $WW$ -fusion diagram being small). Conversely, we define  $\nu_e\bar{\nu}_e\gamma\gamma$  events as  $X\gamma\gamma$  events ( $X = \nu_\ell\bar{\nu}_\ell$ ,  $\ell = e, \mu, \tau$ ) such that  $M_X \geq 130$  GeV. This effectively leaves only the  $WW$ -fusion signal contribution and non- $Z$ -pole background diagrams; interference is again small.

In both the  $Z\gamma\gamma$  and  $\nu_e\bar{\nu}_e\gamma\gamma$  modes, our goal will be to minimize the  $\sigma B(h \rightarrow \gamma\gamma)$  error, defined as  $\sqrt{S+B}/S$ , where  $S$  ( $B$ ) is the number of Higgs signal (background) events. The first important choice is  $\sqrt{s}$ . For the  $Z\gamma\gamma$  channel, the optimal  $\sqrt{s}$  values are given by  $\sqrt{s}_{\text{opt}}(m_{h_{SM}}) \sim 89 \text{ GeV} + 1.25m_{h_{SM}}$  (always close to the peak in the  $Zh_{SM}$  cross section and  $\leq 300$  GeV for  $m_{h_{SM}} \leq 150$  GeV). For the  $\nu_e\bar{\nu}_e\gamma\gamma$  mode, the smallest errors are achieved when  $\sqrt{s}$  is as large as possible. We give results for  $\sqrt{s} = 500$  GeV, at which  $\sqrt{s}$  the  $Z\gamma\gamma$  channel also remains useful. Next are the kinematical cuts. Because of the small signal rates, these cuts must be chosen to reduce the background as much as possible while retaining a large fraction of the Higgs signal events. Keeping in mind the fact that, as a function of  $M_{\gamma\gamma}$ , the Higgs resonance sits on a slowly varying background, a very crucial cut is to accept only events in a small mode-,  $m_{h_{SM}}$ - and detector-resolution-dependent (see later discussion) interval of  $M_{\gamma\gamma}$  centered on  $m_{h_{SM}}$ ,<sup>†</sup> with width chosen so as to minimize  $\sqrt{S+B}/S$ . Additional one-dimensional and two-dimensional kinematic cuts for minimizing the error were extensively investigated.

- For the  $Zh_{SM}$  mode, the best cuts we found are the following:

$$p_T^{\gamma_{1,2}} \geq \frac{m_{h_{SM}}}{4}, \quad p_T^{\gamma_1} + p_T^{\gamma_2} \geq p_T^{\text{min}}(m_{h_{SM}}), \quad (3)$$

where  $p_T^{\gamma_{1,2}}$  are the transverse momenta of the two photons in the  $e^+e^-$  center-of-mass. (By convention,  $E_{\gamma_1} \geq E_{\gamma_2}$ .) Within the statistics of our Monte Carlo study,

---

<sup>†</sup>The Higgs mass will be very precisely measured at the NLC. The background level under the peak will be very precisely normalized using measurements with  $M_{\gamma\gamma}$  away from  $m_{h_{SM}}$ .

the optimal  $p_T^{\min}$  values at  $\sqrt{s} = \sqrt{s}_{\text{opt}}$  ( $\sqrt{s} = 500$  GeV) are given by  $p_T^{\min}(m_{h_{SM}}) \sim 0.9m_{h_{SM}} - 10$  GeV ( $p_T^{\min}(m_{h_{SM}}) \sim 200$  GeV); for such  $p_T^{\min}$ , the photon rapidities are always within  $|y_{\gamma_1}| \leq 1.2$  and  $|y_{\gamma_2}| \leq 1.6$ .

- In the  $\nu_e \bar{\nu}_e h_{SM}$  mode, the smallest error was achieved using the following cuts:

$$\begin{aligned} |y_{\gamma_1}| &\leq 2.5, \quad |y_{\gamma_2}| \leq 2.5, \\ p_T^{\gamma_{1,2}} &\geq p_T^{\gamma_{1,2} \min}(m_{h_{SM}}), \quad p_T^{\gamma_1} + p_T^{\gamma_2} \geq p_T^{\min}(m_{h_{SM}}), \\ p_T^{\text{vis}} &= \sqrt{(p_x^{\gamma_1} + p_x^{\gamma_2})^2 + (p_y^{\gamma_1} + p_y^{\gamma_2})^2} \geq 10 \text{ GeV}. \end{aligned} \quad (4)$$

Within our Monte Carlo statistics, the optimal numerical choices (at  $\sqrt{s} = 500$  GeV) as a function of  $m_{h_{SM}}$  are described by:  $p_T^{\gamma_1 \min}(m_{h_{SM}}) \sim 0.16m_{h_{SM}} + 20$  GeV,  $p_T^{\gamma_2 \min}(m_{h_{SM}}) \sim 0.18m_{h_{SM}} + 1$  GeV, and  $p_T^{\min}(m_{h_{SM}}) \sim 0.5m_{h_{SM}} + 35$  GeV. The  $p_T^{\text{vis}}$  cut is needed to eliminate reducible backgrounds due to events such as  $e^+e^- \rightarrow e^+e^-\gamma\gamma$  where the  $e^+$  and  $e^-$  are lost down the beam pipe leaving the signature of  $\gamma\gamma$  plus missing energy [3].

We note that after the cuts of Eq. (3) or Eq. (4), the photons have substantially different energies, especially in the  $WW$ -fusion case.

Four different electromagnetic calorimeter resolutions are considered: (I) resolution like that of the CMS lead tungstate crystal [4] with  $\Delta E/E = 2\%/\sqrt{E} \oplus 0.5\% \oplus 20\%/E$ ; (II) resolution of  $\Delta E/E = 10\%/\sqrt{E} \oplus 1\%$ ; (III) resolution of  $\Delta E/E = 12\%/\sqrt{E} \oplus 0.5\%$ ; and (IV) resolution of  $\Delta E/E = 15\%/\sqrt{E} \oplus 1\%$ . Cases II and III are at the ‘optimistic’ end of current NLC detector designs [5]. Case IV is the current design specification for the JLC-1 detector [6]. For each resolution case and choice of  $m_{h_{SM}}$ , we determined the  $\Delta M_{\gamma\gamma}$  value which minimizes  $\sqrt{S+B}/S$  in the  $Z\gamma\gamma$  and  $\nu_e \bar{\nu}_e \gamma\gamma$  modes. The optimal  $\Delta M_{\gamma\gamma}$  values for the  $Zh$  mode at  $\sqrt{s} = \sqrt{s}_{\text{opt}}$  and the  $WW$ -fusion mode at  $\sqrt{s} = 500$  GeV are the same within Monte Carlo errors:  $\Delta M_{\gamma\gamma}(\text{I, II, III, IV})(\text{GeV}) \sim (0.015, 0.035, 0.035, 0.045)m_{h_{SM}}$ . For  $Zh_{SM}$  production at  $\sqrt{s} = 500$  GeV,  $\sqrt{S+B}/S$  is minimized for  $\Delta M_{\gamma\gamma}(\text{I, II, III, IV}) \sim (0.015, 0.03, 0.03, 0.04)m_{h_{SM}}$ .

The optimal  $\Delta M_{\gamma\gamma}$ ,  $p_T^{\min}$ , and  $p_T^{\gamma_{1,2} \min}$  values specified above are ‘soft’; changes in the  $p_T$  cuts by  $\pm 5$  GeV or in  $\Delta M_{\gamma\gamma}/m_{h_{SM}}$  by  $\pm 0.005$  lead to  $\leq 0.01$  change in  $\sqrt{S+B}/S$ .

### III. RESULTS AND DISCUSSION

The first two windows of Figure 1 show the statistical errors,  $\sqrt{S+B}/S$ , for measuring  $\sigma B(h_{SM} \rightarrow \gamma\gamma)$  in the  $Z^* \rightarrow Zh_{SM}$  and  $\nu_e \bar{\nu}_e h_{SM}$  ( $WW$ -fusion) measurement modes as a function of  $m_{h_{SM}}$ . We assume four years of  $L = 50 \text{ fb}^{-1}/\text{yr}$  running, *i.e.*  $L = 200 \text{ fb}^{-1}$ , at  $\sqrt{s} = \sqrt{s}_{\text{opt}}$  ( $\sqrt{s} = 500 \text{ GeV}$ ) in the  $Zh_{SM}$  ( $WW$ -fusion) cases, respectively. Comparing, we find that in resolution cases II-IV the  $Zh_{SM}$  ( $WW$ -fusion) measurement mode yields smaller errors for  $70 \lesssim m_{h_{SM}} \lesssim 120 \text{ GeV}$  ( $130 \lesssim m_{h_{SM}} \lesssim 150 \text{ GeV}$ ). In resolution case I, the  $Zh_{SM}$  mode error is the smaller for masses up to 130 GeV. As a function of  $m_{h_{SM}}$ , the smallest errors are obtained for  $100 \text{ GeV} \lesssim m_{h_{SM}} \lesssim 130 \text{ GeV}$ .<sup>‡</sup> For calorimeter resolutions II or III, the errors range from  $\pm 25\%$  to  $\pm 29\%$  for the ( $\sqrt{s} = \sqrt{s}_{\text{opt}}$ )  $Zh_{SM}$  measurement and from  $\pm 26\%$  to  $\pm 33\%$  for the ( $\sqrt{s} = 500 \text{ GeV}$ )  $WW$ -fusion measurement.

In the third window of Fig. 1 we plot the error obtained by combining the  $WW$ -fusion and  $Zh_{SM}$  mode  $\sigma B(h_{SM} \rightarrow \gamma\gamma)$  statistics for  $L = 200 \text{ fb}^{-1}$  accumulated at  $\sqrt{s} = 500 \text{ GeV}$ .<sup>§</sup> This is close to the error for  $B(h_{SM} \rightarrow \gamma\gamma)$  obtained by combining the two ratios in Eq. (2) given that errors for the other inputs are much smaller than the  $\sigma B(h_{SM} \rightarrow \gamma\gamma)$  errors. Although the  $Zh_{SM}$  mode error at  $\sqrt{s} = 500 \text{ GeV}$  is always larger than the  $WW$ -fusion mode error, including the  $Zh_{SM}$  measurement substantially improves the net  $B(h_{SM} \rightarrow \gamma\gamma)$  error relative to that obtained using  $WW$ -fusion alone, especially at low  $m_{h_{SM}}$ . For  $100 \text{ GeV} \lesssim m_{h_{SM}} \lesssim 130 \text{ GeV}$ , the net error ranges from  $\pm 23\%$  to  $\pm 27\%$ .

Although observation of a clear Higgs signal in the  $\gamma\gamma$  invariant mass distribution is not

---

<sup>‡</sup>In the MSSM the light Higgs has  $m_{h^0} \lesssim 130 \text{ GeV}$ .

<sup>§</sup>We do not discuss the reverse situation, since the  $WW$ -fusion rate at  $\sqrt{s}_{\text{opt}}$  is always  $\lesssim 1/5$  of that for  $Zh_{SM}$ .

an absolute requirement (given that we will have observed the  $h_{SM}$  in other channels and will have determined its mass very accurately) it would be helpful in case there is significant systematic uncertainty in measuring the  $\gamma\gamma$  invariant mass. It is vital to be certain that the  $\Delta M_{\gamma\gamma}$  interval is centered on the mass region where the Higgs signal is present. Taking  $\sqrt{s} = \sqrt{s}_{\text{opt}}$  ( $\sqrt{s} = 500 \text{ GeV}$ ) for the  $Zh_{SM}$  ( $WW$ -fusion) mode and  $L = 200 \text{ fb}^{-1}$ , we find  $S/\sqrt{B} \geq 3$  in the following (resolution-dependent) regions:

$$\begin{aligned}
&\text{case I : } 70 \leq m_{h_{SM}} \leq 150 \text{ GeV } (Zh_{SM}), \quad 80 \leq m_{h_{SM}} \leq 150 \text{ GeV } (WW\text{--fusion}), \\
&\text{cases II/III : } 80 \leq m_{h_{SM}} \leq 140 \text{ GeV } (Zh_{SM}), \quad 90 \leq m_{h_{SM}} \leq 150 \text{ GeV } (WW\text{--fusion}) \quad (5) \\
&\text{case IV : } 90 \leq m_{h_{SM}} \leq 130 \text{ GeV } (Zh_{SM}), \quad 100 \leq m_{h_{SM}} \leq 150 \text{ GeV } (WW\text{--fusion}),
\end{aligned}$$

#### IV. FINAL REMARKS AND CONCLUSIONS

We have studied the prospects for measuring  $\sigma B(h \rightarrow \gamma\gamma)$  for a SM-like Higgs boson, with  $70 \leq m_{h_{SM}} \leq 150 \text{ GeV}$ , at the NLC. The measurements will be challenging but of great importance. We have compared results for two different production/measurement modes:  $Z^* \rightarrow Zh$  and  $WW$ -fusion. Errors for the  $WW$ -fusion channel are minimized at full machine energy,  $\sqrt{s} = 500 \text{ GeV}$ . Errors in the  $Zh$  channel are minimized if the machine energy is tuned to the ( $\leq 300 \text{ GeV}$ )  $\sqrt{s} = \sqrt{s}_{\text{opt}}$  value which maximizes the  $Zh$  event rate. The net error for  $B(h_{SM} \rightarrow \gamma\gamma)$  is approximately given by combining the  $WW$  and  $Zh$  channel  $\sigma B$  errors, since errors for other quantities entering the ratios of Eq. (2) are small. At  $\sqrt{s} = 500 \text{ GeV}$ , the error obtained using only the  $WW$ -fusion channel measurement is significantly decreased by including the  $Zh$  channel measurement. At  $\sqrt{s} = \sqrt{s}_{\text{opt}}$ , the  $WW$ -fusion channel can be neglected and the net error is essentially just that for the  $Zh$  channel. At any  $\sqrt{s}$  and in either channel, the better the electromagnetic calorimeter resolution, the smaller the error in  $B(h_{SM} \rightarrow \gamma\gamma)$ . For  $100 \leq m_{h_{SM}} \leq 130 \text{ GeV}$ , where  $B(h_{SM} \rightarrow \gamma\gamma)$  is largest (a mass range that is also highly preferred for the light SM-like  $h^0$  of the MSSM), and  $L = 200 \text{ fb}^{-1}$ , the net error assuming an excellent CMS-style calorimeter (resolution

case I) falls in the ranges  $\sim \pm 18\%$  to  $\sim \pm 20\%$  at  $\sqrt{s} = \sqrt{s}_{\text{opt}}$  and  $\sim \pm 18\%$  to  $\sim \pm 22\%$  at  $\sqrt{s} = 500 \text{ GeV}$ . For  $L = 200 \text{ fb}^{-1}$  and a calorimeter at the optimistic end of current plans for the NLC detector (cases II and III), the  $100 \leq m_{h_{SM}} \leq 130 \text{ GeV}$  net error falls in the ranges  $\sim \pm 25\%$  to  $\sim \pm 29\%$  at  $\sqrt{s} = \sqrt{s}_{\text{opt}}$  and  $\sim \pm 22\%$  to  $\sim \pm 27\%$  at  $\sqrt{s} = 500 \text{ GeV}$ .

If the NLC is first operated at  $\sqrt{s} = 500 \text{ GeV}$ , either because a Higgs boson has not been detected previously or because other physics (*e.g.* production of supersymmetric particles) is deemed more important, data will be accumulated with whatever calorimeter is part of the initial detector and a corresponding measurement of  $B(h_{SM} \rightarrow \gamma\gamma)$  will result. The desirability of stopping data collection to upgrade the calorimeter and/or reconfigure the interaction region for full luminosity at the  $Zh_{SM}$  cross section maximum must be carefully evaluated.\*\* Using the  $L = 200 \text{ fb}^{-1}$  errors of Fig. 1, we find that it is *not* advantageous to reconfigure for  $\sqrt{s} = \sqrt{s}_{\text{opt}}$  if  $m_{h_{SM}} \gtrsim 100 \text{ GeV}$ . The value of a calorimeter upgrade is also marginal for such  $m_{h_{SM}}$ . To illustrate, suppose the initial calorimeter has resolution II or III. For  $m_{h_{SM}} = 120 \text{ GeV}$ , upgrading the calorimeter from II/III to I, and then accumulating a 2nd  $L = 200 \text{ fb}^{-1}$  at  $\sqrt{s} = 500 \text{ GeV}$  after doing so, would yield a net  $B(h_{SM} \rightarrow \gamma\gamma)$  error of  $\pm 14\%$ , as compared to  $\sim \pm 15.5\%$  if no changes are made and a total of  $L = 400 \text{ fb}^{-1}$  is accumulated by simply running twice as long. For  $m_{h_{SM}} = 150 \text{ GeV}$ , upgrading the resolution would yield (after the 2nd  $L = 200 \text{ fb}^{-1}$  run at  $\sqrt{s} = 500 \text{ GeV}$ )  $\sim \pm 22\%$  error vs.  $\sim \pm 25\%$  if no calorimeter change is made. However, for small  $m_{h_{SM}}$ , reconfiguration and high resolution calorimetry both become quite valuable at the NLC. For example, if  $m_{h_{SM}} = 70 \text{ GeV}$  (roughly the current LEP I/II limit), a 2nd  $L = 200 \text{ fb}^{-1}$  run with full  $\mathcal{L}$  at  $\sqrt{s} = \sqrt{s}_{\text{opt}}$  and upgrade to resolution I would yield  $\sim \pm 24\%$  error vs.  $\sim \pm 38\%$  after a 2nd  $L = 200 \text{ fb}^{-1}$  run with no changes. For  $m_{h_{SM}} = 70 \text{ GeV}$ , running from the beginning for  $L = 400 \text{ fb}^{-1}$  at the  $\sigma(Zh_{SM})$  peak (as possible at full luminosity if  $m_{h_{SM}}$  is known from

---

\*\*It is best to continue to run at  $\sqrt{s} = 500 \text{ GeV}$  if the interaction region is not reconfigured for full luminosity at the lower  $Zh_{SM}$ -channel  $\sqrt{s}_{\text{opt}}$ .



LHC data) with resolution I yields error of  $\sim \pm 19\%$ .

In evaluating different options/strategies, it is necessary to keep in mind that LHC data may allow a rather competitive error for  $B(h_{SM} \rightarrow \gamma\gamma)$  [1]. One combines the  $L = 600 \text{ fb}^{-1}$  (for ATLAS and CMS combined) LHC measurement of  $B(h_{SM} \rightarrow \gamma\gamma)/B(h_{SM} \rightarrow b\bar{b})$  with the  $L = 200 \text{ fb}^{-1}$ ,  $\sqrt{s} = 500 \text{ GeV}$  NLC measurement of  $B(h_{SM} \rightarrow b\bar{b})$  to obtain a value for  $B(h_{SM} \rightarrow \gamma\gamma)$  with error  $\sim \pm 16\%$  for  $80 \leq m_{h_{SM}} \leq 130 \text{ GeV}$ , rising to  $\sim \pm 25\%$  for  $m_{h_{SM}} \sim 140 \text{ GeV}$ . If we combine this  $B(h_{SM} \rightarrow \gamma\gamma)$  error with the net error for the ( $Zh_{SM}$  plus  $WW$ -fusion mode,  $\sqrt{s} = 500 \text{ GeV}$ ,  $L = 200 \text{ fb}^{-1}$ , resolution II/III) direct  $B(h_{SM} \rightarrow \gamma\gamma)$  measurement at the NLC, the overall error for  $B(h_{SM} \rightarrow \gamma\gamma)$  will be:

$m_{h_{SM}} \text{ (GeV)}$	80	100	110	120	130	140	150
Error	$\pm 15\%$	$\pm 14\%$	$\pm 13\%$	$\pm 13\%$	$\pm 13\%$	$\pm 18\%$	$\pm 35\%$

For most Higgs masses, there would be little to gain from excellent (case I) resolution. For example, at  $m_{h_{SM}} \sim 120 \text{ GeV}$ , the above  $\sim \pm 13\%$  found assuming NLC resolution cases II/III would only improve to  $\sim \pm 12\%$  for NLC resolution case I. For  $m_{h_{SM}} \sim 80 \text{ GeV}$ , the NLC  $h_{SM} \rightarrow \gamma\gamma$  decay determination of  $B(h_{SM} \rightarrow \gamma\gamma)$  will only be of value if  $L = 400 \text{ fb}^{-1}$  with calorimeter resolution I can be accumulated by the time  $L = 300 \text{ fb}^{-1}$  per detector is accumulated at the LHC. Finally, if determining  $\Gamma_{h_{SM}}^{\text{tot}}$ , and thence  $\Gamma(h_{SM} \rightarrow b\bar{b})$ , is the dominant motivation for measuring  $B(h_{SM} \rightarrow \gamma\gamma)$ , then it is important to note that for  $m_{h_{SM}} \gtrsim 130 \text{ GeV}$   $\Gamma_{h_{SM}}^{\text{tot}}$  is better determined using the  $h_{SM} \rightarrow WW^*$  techniques discussed in Ref. [1]. For such  $m_{h_{SM}}$ , this fact and the small gain in  $B(h_{SM} \rightarrow \gamma\gamma)$  error (especially if LHC data is available) argue against considering a calorimeter upgrade.

## V. ACKNOWLEDGEMENTS

This work was supported in part by Department of Energy under grant No. DE-FG03-91ER40674 and by the Davis Institute for High Energy Physics. We would like to thank T. Barklow, J. Brau, P. Rowson, R. Van Kooten and L. Poggioli for helpful communications.

## REFERENCES

- [1] J.F. Gunion, L. Poggioli and R. Van Kooten, *Higgs Boson Discovery and Properties*, hep-ph/9703330, to appear in *Proceedings of the 1996 DPF/DPB Summer Study on "New Directions in High Energy Physics" (Snowmass, 96)*, June 25 - July 12, 1996, Snowmass, Colorado.
- [2] See J.F. Gunion, A. Stange, and S. Willenbrock, *Weakly-Coupled Higgs Bosons*, preprint UCD-95-28 (1995), to be published in *Electroweak Physics and Beyond the Standard Model*, World Scientific Publishing Co., eds. T. Barklow, S. Dawson, H. Haber, and J. Siegrist, a references therein.
- [3] C.-H. Chen, M.Drees, and J.F. Gunion, Phys. Rev. Lett. **76**, 2002 (1996).
- [4] CMS Technical Proposal, CERN/LHCC 94-38 (1994).
- [5] *Physics and Technology of the Next Linear Collider: a Report Submitted to Snowmass 1996*, BNL 52-502, p. 25; see also the simulation homepage: [http:// nlc.physics.upenn.edu /nlc /software /software.html](http://nlc.physics.upenn.edu/nlc/software/software.html).
- [6] JLC-I, JLC Group, KEK Report 92-16, as summarized by K. Fujii, *Proceedings of the 2nd International Workshop on "Physics and Experiments with Linear  $e^+e^-$  Colliders"*, eds. F. Harris, S. Olsen, S. Pakvasa and X. Tata, Waikoloa, HI (1993), World Scientific Publishing, p. 782.

# FIGURES

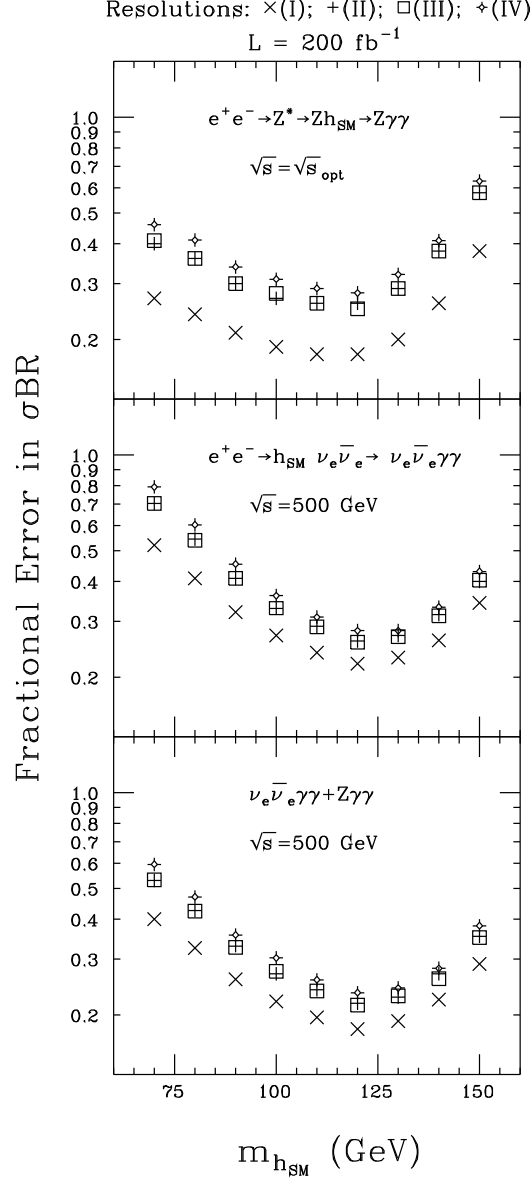


FIG. 1. The fractional error in the measurement of  $\sigma(\nu_e \bar{\nu}_e h_{SM})B(h_{SM} \rightarrow \gamma\gamma)$  (at  $\sqrt{s} = 500 \text{ GeV}$ ) and  $\sigma(Zh_{SM})B(h_{SM} \rightarrow \gamma\gamma)$  (at  $\sqrt{s} = \sqrt{s}_{\text{opt}}$ ) as a function of  $m_{h_{SM}}$  assuming  $L = 200 \text{ fb}^{-1}$ . Also shown is the fractional  $\sigma B(h_{SM} \rightarrow \gamma\gamma)$  error obtained by combining  $Zh_{SM}$  and  $\nu_e \bar{\nu}_e h_{SM}$  channels for  $L = 200 \text{ fb}^{-1}$  at  $\sqrt{s} = 500 \text{ GeV}$ . Results for the four electromagnetic calorimeter resolutions described in the text are given.